Journal of Structural Geology 32 (2010) 192–201

Contents lists available at ScienceDirect

Journal of Structural Geology

journal homepage: www.elsevier.com/locate/jsg

Hybrid veins from the southern margin of the Bristol Channel Basin, UK

Mandefro Belayneh*, John W. Cosgrove

Imperial College London, Department of Earth Science and Engineering, Royal School of Mines, Exhibition Road, London SW7 2AZ, United Kingdom

ARTICLE INFO

Article history:
Received 9 April 2009
Received in revised form
29 October 2009
Accepted 10 November 2009
Available online 7 December 2009

Keywords:
Hybrid veins
Transtensional
Bristol Channel Basin

ABSTRACT

Sinistral and dextral *en echelon* hybrid calcite veins are exposed on the southern margin of the Bristol Channel Basin, North Somerset on a Liassic carbonate platform. These hybrid veins are transitional between pure extensional (mode I) and shear fractures (mode II, mode III) and experienced both extensional and shear displacements during their formation. In the study area they occur in conjugate sets with the conjugate angle ranging between 10° and 50°. Based on the kinematic analysis of these veins a new model for the opening of the Bristol Channel is proposed.

1. Introduction

Pollard and Aydin (1988) define joints as the subset of fractures which show evidence of only opening mode displacement, *i.e.* mode I fracture formed by extension. Others, for example, Price (1966) and Hancock (1985) define joints as a surface along which there has been no appreciable displacement. The latter definition allows all fractures (mode I, mode II, mode III and mixed-mode) to be classified as joints as long as the displacements are small. In subsiding sedimentary basin where fluids enriched with dissolved minerals are abundant, barren fractures can often be filled with minerals such as calcite and quartz. Although Peacock (2004) proposed that joints and veins should be analysed separately, attributes of fractures and veins can be analysed in the same way. For example, the mechanical and statistical approaches proposed by Nelson (1985) for the analysis of fractures can also be applied to veins to determine the stress history linked to the formation of the various vein sets and to study their initiation, their propagation, coalescence and mechanical interaction. Likewise, the statistical approach to fracture analysis which attempts to relate the different fracture distribution patterns to the mechanisms of their formation (Hudson and Priest, 1979; Priest and Hudson, 1976, 1981; Sen and Kazi, 1984; Huang and Angelier, 1989; Narr and Suppe, 1991; Rives et al., 1992; Odling, 1997; Odling et al., 1999; Gillespie et al., 1993, 2001; van Djik et al., 2000) can be used to analyse veins and dykes (see *e.g.* Pollard and Segall, 1987; Jolly and Sanderson, 1995; Vermilye and Scholz, 1995; Jolly et al., 1998; Ryan et al., 2000; Belayneh et al., 2006). The study of veins is important because in addition to providing the data usually used in fracture analysis (geometry, orientation and distribution) they often provide, in the form of fibrous mineral infill, information relating to the displacements associated with their formation. In addition, minerals crystallizing in the presence of fluids may trap fluid inclusions which can be used to determine the fluid composition and the pressure and temperature conditions at the time of vein formation.

Experiments on brittle failure show two fundamentally different types of fractures: extension fractures (mode I) and shear fractures (modes II and III) (see *e.g.* Atkinson, 1987; Twiss and Moores, 1992). The combination of any of the above modes of crack displacement gives rise to mixed-mode failure. The brittle failure criterion can be graphically expressed as a composite Griffith and Navier–Coulomb criteria (Fig. 1a) and the type of brittle failure, whether extension or shear, is determined by the magnitude of differential stress (*e.g.* Anderson, 1951; Price and Cosgrove, 1990). The formation of shear fractures requires a differential stress greater than four times the tensile strength, *T*, and the formation of extensional fractures a differential stress less than four times the tensile strength. Joints form parallel to σ_1 (Fig. 1a(iii)) and normal to σ_3 and shear fractures form as conjugate sets approximately 30° on either side of the σ_1/σ_2 plane, (Fig. 1a(v)). These geometric relationships between the different fracture types and their causative stress field, form the basis of fracture analysis. An examination of the combined

* Corresponding author. Tel./fax: +44 020 75946463.
E-mail address: m.belayneh@imperial.ac.uk (M. Belayneh).

0191-8141/$ – see front matter
doi:10.1016/j.jsg.2009.11.010

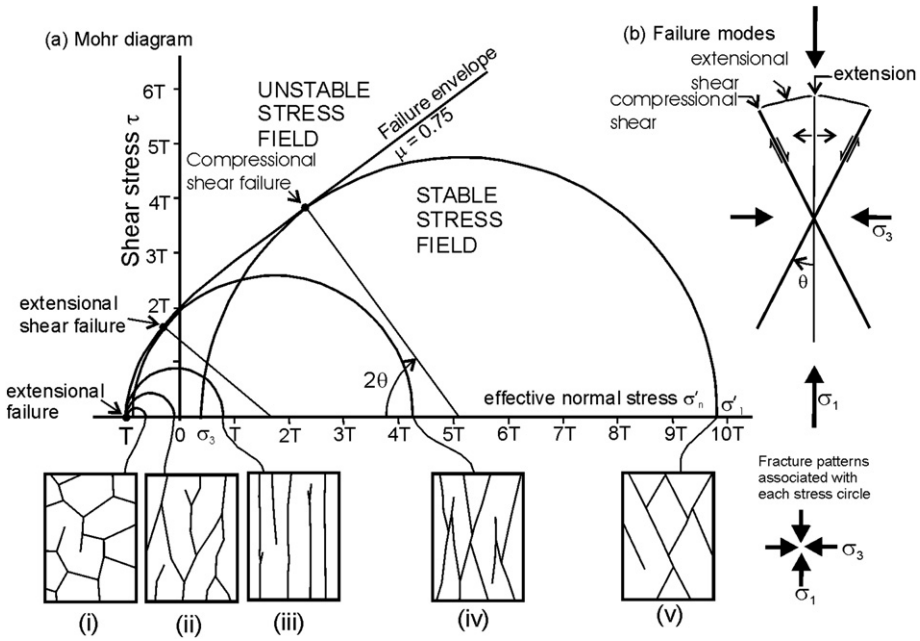

Fig. 1. (a) Navier–Coulomb–Griffith combined extensional and shear brittle failure envelope showing five stress states all of which will cause failure, (i)–(iii) have a low differential stress (<4 T) and result in extensional failure, (v) has a large differential stress and results in shear failure, (iv) has a differential stress around 4 T and results in hybrid failure. (b) Summary diagram showing the relationship between the types of failure and the causative stress field (taken from Woodcock et al., 2007 modified from Cosgrove, 1995).

Griffith and Navier–Coulomb criterion indicates that there is a transition from shear to extensional fractures through an intermediate fracture type referred to in this work as 'hybrid' fractures. These fractures show both extensional and shear displacements (Fig. 1a(iv)). The hybrid fractures range in orientation between that of extensional fractures and that of shear fractures. Although it is clear from the Griffith Mohr–Coulomb criteria that they form when the differential stress is approximately 4 T, the factors leading to their formation remain largely unclear (see *e.g.* the discussion by Engelder, 1999 who questioned their existence).

Experiments conducted on Carrara Marble by Ramsay and Chester (2004) and Rodriguez (2005) show brittle structures ranging from joints (opening mode) via hybrid fractures to shear fractures. The experiments show that at low maximum compressive stress (7.5–60 MPa), the extension fractures display somewhat undulating, discrete, highly reflective calcite cleavage planes at sample scale and show roughness at grain scale. At intermediate compressive stress (70–120 MPa), the fractures are inclined between 3° and 10° to σ_1 and they exhibit patches of discrete, reflective and cleaved crystals between fault gouges showing slip lineation. At high maximum compressive stress (130–170 MPa), the fractures are inclined between 13° and 22° to σ_1. Gouges with grooves and striations formed declaring the down-dip slip direction on these fractures. This experimental work revealed a progressive increase of fracture angle, θ (Fig. 1), with differential stress and generated a complete range of fractures from extension to shear fractures via hybrid fractures. Bobich (2005) carried out a similar triaxial experiment on Berea Sandstone and reported a transition from tensile to shear fractures via hybrid fractures when σ_1 is approximately 50 MPa.

A variety of terms have been used by structural geologists to describe these structures including hybrid extension/shear fractures (Price and Cosgrove, 1990), extensional-shear (Sibson, 1996, 1998, 2003), hybrid joints (Bahat, 1991; Hancock, 1994; Marín-Lechado et al., 2004), hybrid fracture (Ferrill et al., 2004), mixed-mode fractures (Twiss and Moores, 1992), transitional tensile (Suppe, 1985) and transitional fractures (van der Pluijm and Marshak, 1997; Engelder, 1999).

In a study of naturally occurring conjugate sets of *en echelon* tension gashes, Smith (1996) recognised that these systems could be classified in terms of two parameters. These are: (i) the angle between the two arrays of *en echelon* tension gashes, 2θ in Fig. 2a *i.e.* the conjugate angle, and (ii) the angle between the individual tension gashes and the array of *en echelon* tension gashes of which it is a part, α (Fig. 2b) *i.e.* the vein array angle.

As briefly noted above, within the context of fracture analysis the most useful indicators of stress orientation are the fractures themselves. Joints form normal to the least principal compressive stress, σ_3, *i.e.* parallel to the plane containing the maximum and intermediate principal stresses and conjugate shear fractures form symmetrically about the maximum principal compressive stress σ_1. These geometric relationships enable the orientation of the principal stresses to be determined. In addition, the mineral infill of some veins is fibrous and the fibres show the direction of opening.

Conjugate shear fractures are often initiated as two sets of *en echelon* extensional fractures (Fig. 2a) filled with vein material (see *e.g.* Ramsay, 1967; Ramsay and Huber, 1987). Theoretically the extension veins in both sets should be parallel to each other and to the applied maximum principal compressive stress which bisects the acute angle between the sets (see *e.g.* array (ii) Fig. 2b). However, sets are often found in which the extensional veins in the conjugate sets either converge or diverge, Fig. 2b. In addition, these veins can have straight, pinnate, or sigmoidal geometries. Pinnate veins are a set of *en echelon* veins linked to and propagating away from a shear fracture at a small angle (Wilson, 1961). Sigmoidal vein shapes indicate concurrent fracture propagation and shear strain (Durney and Ramsay, 1973) and the veins can display an S- or Z-geometry (Fig. 2a). Veins can form by repeated opening and sealing, *i.e.* the mechanism of crack-seal proposed by Ramsay (1980) (see also Ramsay and Huber, 1987; Urai et al., 1991; Nicholson, 1991) or by the

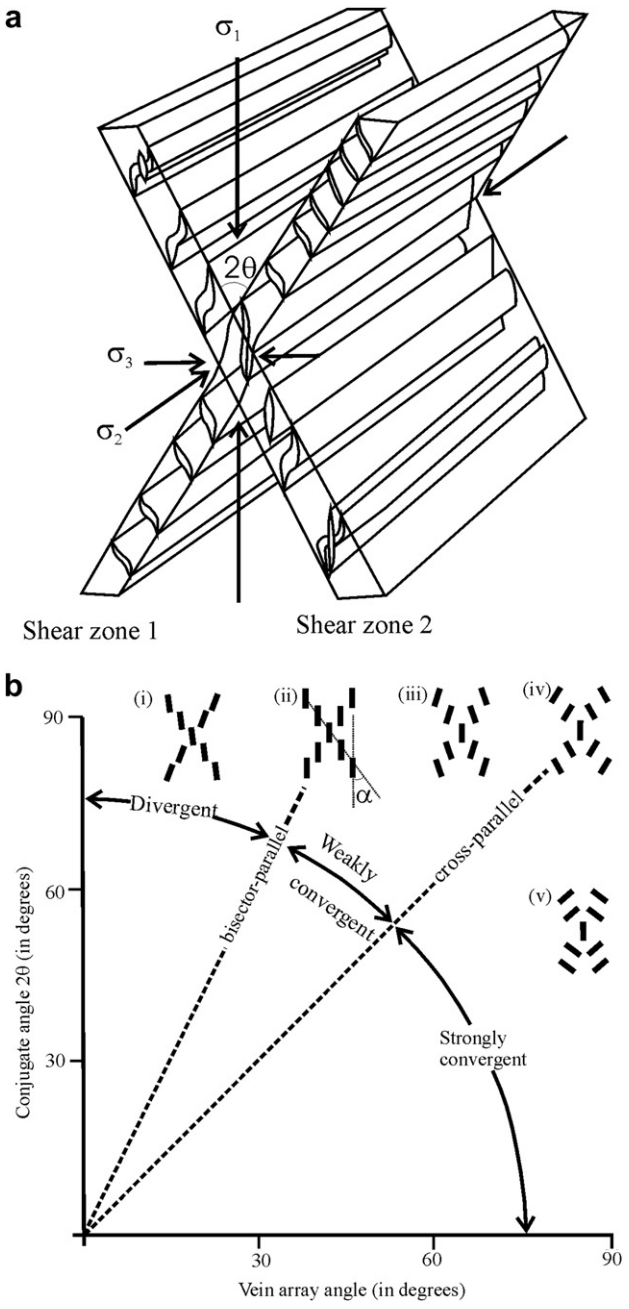

Fig. 2. (a) Three dimensional schematic diagram of *en echelon* veins in conjugate shear zones (redrawn from Ramsay and Huber, 1987, their Fig. 26.39), (b) a plot of conjugate angle (2θ) versus vein array angle (α) of conjugate *en echelon* veins showing (i) divergent, (ii) bisector-parallel, (iii–iv) cross-parallel, convergent vein arrays. (iv) A special case of a convergent vein array in which the veins in one array are parallel to the enveloping surface of conjugate vein array (modified from Smith, 1996, Fig. 2).

"crack-jump" mechanism proposed by Caputo and Hancock (1999). From our field observations, the veins considered in this study, which, as will be discussed later, formed during the opening of the Bristol Channel Basin, do not show evidence for the repeated opening and sealing that characterises the crack-seal mechanism. However, there are veins in the study area post-dating the veins considered in this study which probably formed as a result of crack-seal during basin inversion. These veins contain slivers of the country rock, and the calcite that fills the veins is fibrous with fibres normal to the bedding parallel vein walls. These veins are not considered in this study.

Various models have been proposed for the opening and subsequent inversion of the Bristol Channel Basin. Nemčok and Gayer (1996) studied the northern margin of the basin and concluded that a consistently NE–SW oriented σ_3 occurred from the Late Triassic to Early Cretaceous. Peacock and Sanderson (1999) and Peacock (2004) presented a more complex history for the evolution of the basin based mainly on studies on the southern margin of the basin. Their proposed history involves the following stages; (1) a 150° directed extension that led to the formation of 060° striking extension veins, joints and normal faults (2) a N–S extension which produced sinistral transtension on pre-existing 095° striking normal faults and veins, (3) an E–W contraction with sinistral shear on some of the 095° striking normal faults (sic., we note that this contraction would in fact generate dextral transpression on 095° striking faults, *i.e.* as described in stage 4), (4) a dextral reactivation of some of the 095° striking normal faults, (5) a N–S contraction which led to reverse reactivation of the 095° striking normal faults and to the development of thrusts faults. Al Mahruqi (2001) reported ~N–S oriented, right-stepping strike-slip faults locally displacing these later joints.

The present paper discusses the first four events listed above and attempts to account for their formation in terms of a single ~N–S extension. This analysis is based on the use of two types of kinematic indicators, namely *en echelon* tension gashes and mineral fibres.

In the following section the geology and structural evolution of the study area is briefly reviewed and a description of some examples of hybrid veins cropping out east of Lilstock on the southern margin of the Bristol Channel Basin (Fig. 3) is presented. This is followed by a brief discussion and conclusion.

2. Geology and structures

The study area is located on the southern margin of the Bristol Channel, North Somerset, UK (Fig. 3). The rift-related, approximately E–W trending Bristol Channel Basin was initiated in the Permian–Triassic (Kamerling, 1979; van Hoorn, 1987; Brooks et al., 1988; Nemčok et al., 1995; Rawnsley et al., 1998). Rifting continued throughout the Jurassic into the Early Cretaceous (Dart et al., 1995; Nemčok and Gayer, 1996). The oldest beds in this basin are represented by the Lower Triassic succession of red marls with interbedded sandstones and evaporites passing upwards into the marine sediments of the Lower Lias consisting of alternating limestone beds and marls.

Early lithification of the Liassic carbonate beds made them susceptible to brittle deformation. Small-scale polygonal fractures with triple junctions were locally formed and are probably related to dewatering of the sediments during the early stages of burial and compaction. These were followed by the formation of E–W to WNW–ESE striking, closely spaced, bed-normal high density veins (Rawnsley et al., 1998) or micro-veins (Caputo and Hancock, 1999) crosscutting the polygonal fractures and which formed as a result of a brittle response to a regional, approximately N–S stretching. The vertical extent of these layer-normal joints which are filled with microcrystalline calcite is determined by the thickness of individual limestone beds. Initially the rate of opening and mineral precipitation was approximately balanced. Some of these embryonic veins gradually developed into the 'early veins' (the main focus of this work) which as noted below, are linked to the formation of major faults. As basin opening continued, further extension resulted in the oblique linkage of appropriately positioned joints in adjacent limestone beds by shear fractures that developed in the intervening shales. Progressive extension and basin subsidence caused slip on these composite, stepped fractures that acted as WNW–ESE striking normal faults resulting in the formation of pull-apart-voids

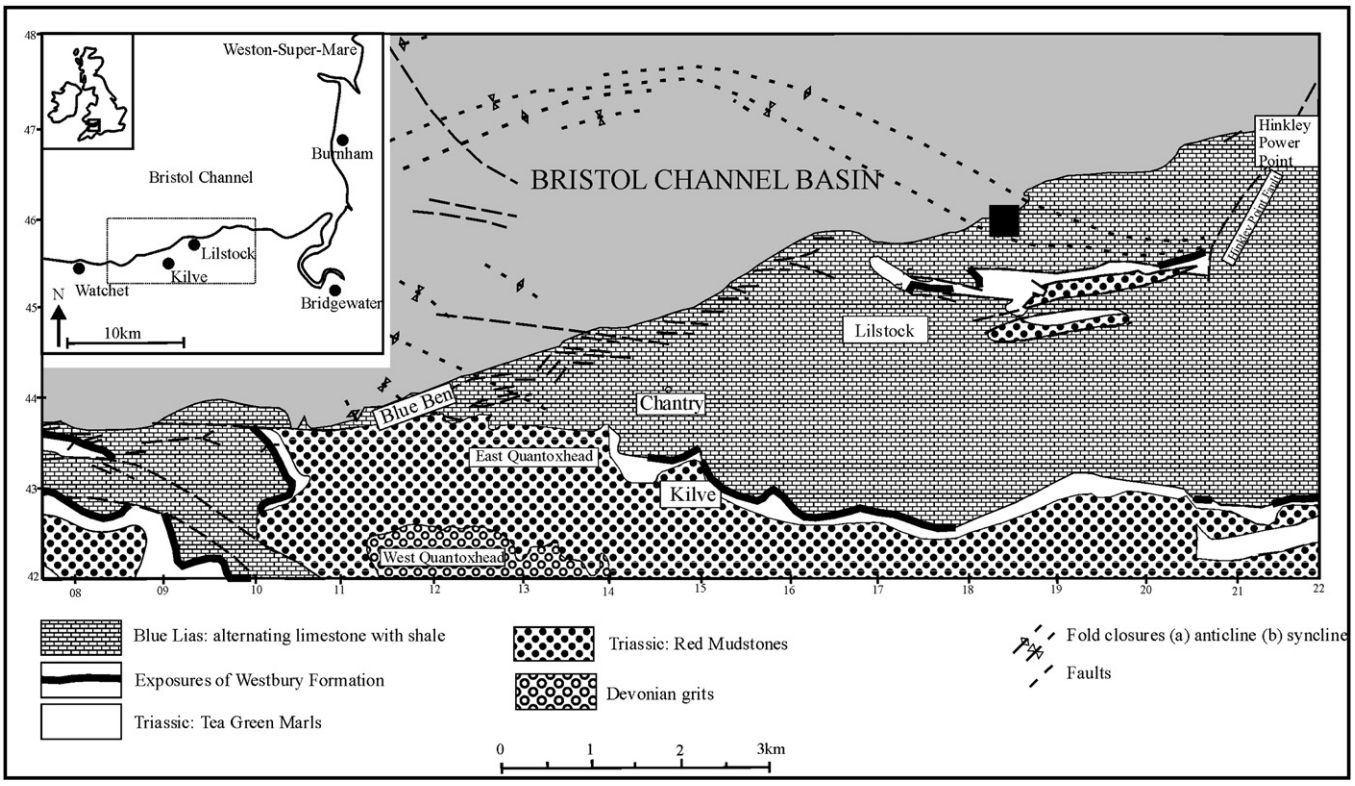

Fig. 3. Location map of the study area on the southern margin of the Bristol Channel (modified from 1:50,000 scale geological maps of England and Wales, sheets 279, and parts of sheets 263 and 295). The inset map shows the location of the Bristol Channel Basin and the black rectangle shows the location of the study area.

in the limestones (see Davison, 1995; Belayneh and Cosgrove, 2004). The veins commonly observed on the southern margin of the Bristol Channel Basin are approximately sub-parallel to the micro-veins and occasionally intersect them at angle between 5° and 10°.

3. Results

This section describes some key observations which are used to present a new interpretation of the evolution of the opening of the Bristol Channel Basin. The majority of veins in the study area are aligned parallel to the ~E–W striking normal faults.

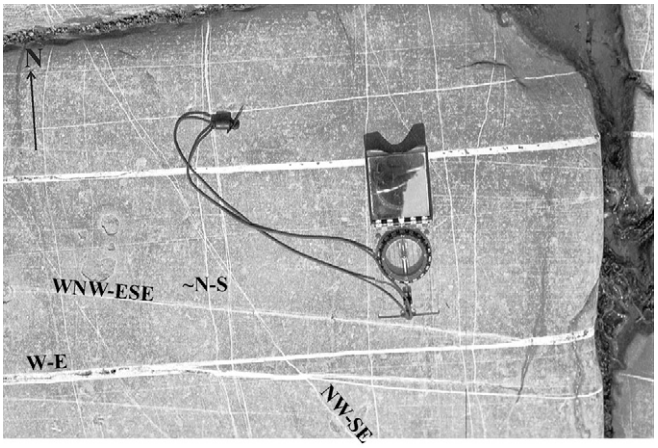

Fig. 4. Four vein sets are shown chronologically starting with the oldest: WNW–ESE, E–W, NW–SE and ~N–S. The E–W vein set is the most abundant in the area.

Four vein sets are shown in Fig. 4. The chronological order is established based on crosscutting relationships starting with the oldest WNW–ESE, ~E–W, NW–SE and ~N–S. The veins within each set are sub-parallel to each other. The WNW–ESE set represent the embryonic veins (micro-veins). The ~E–W vein set is the most abundant in the study area. The NW–SE vein set is restricted mainly to the east of Lilstock (Fig. 3) (see Belayneh et al., 2006) and the N–S set is commonly observed in the vicinity of the conjugate NW–SE dextral and NE–SW sinistral strike-slip faults.

As noted above, opening mode veins are more abundant than those veins showing sinistral and dextral sense of displacement. These veins are generally sub-parallel to the basin bounding faults. However, as shown in Fig. 5a there are also places where these veins occur in a left-stepping and right-stepping *en echelon* pattern. The conjugate sets of *en echelon* veins shown in Fig. 5a and b are each made up of individual tension gashes which show planar and sigmoidal shapes (Fig. 2a). The individual veins display a cross-parallel geometry (see (iv) in Fig. 2b). One of the two shear zones defined by these *en echelon* vein sets striking between 250° and 270° the other between 300° and 320°. Both are sub-vertical. The bisector of the acute dihedral angle trends approximately 285° and the acute angle between the conjugate shear zones (2θ) ranges between 10° and 50°. This configuration is not characteristic of joints that form in pure open mode displacement where $2\theta = 0$ or shear fractures forming at approximately 30° either side of the maximum principal compressive stress. The hybrid (extension/shear) fractures (Fig. 1(iv)) formed in the region of $0 \leq 2\theta \leq 60°$.

Field observations show that the two conjugate arrays making up the hybrid system of fractures are not developed to the same extent.

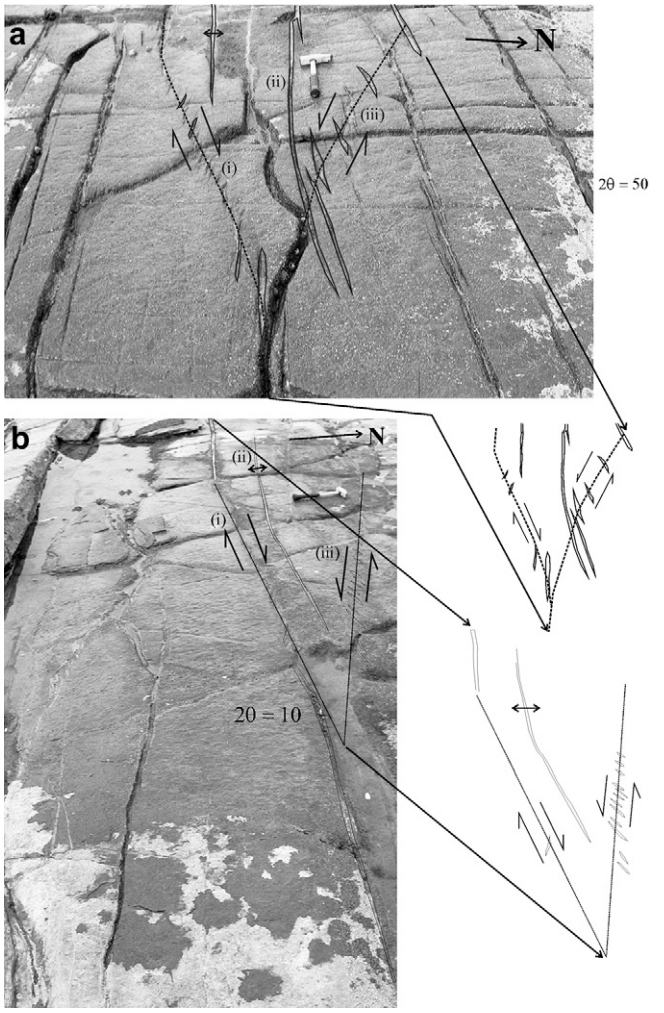

Fig. 5. Conjugate hybrid veins consisting of left- and right-stepping *en echelon* veins with acute bisector of a 50° (a) and 10° (b). In the lower photograph, the shear zones strike 270° and 280°. Veins show both straight and incipient sigmoidal Z- and S-shapes indicating shear strain accompanying their propagation. The veins are sub-vertical and normal to the bedding. (i) Left-stepping *en echelon* veins indicating a dextral sense of displacement, (ii) veins sub-parallel to the bisector of the acute angle. The calcite fibres are normal to the fracture wall showing an opening mode displacement, and (iii) right-stepping *en echelon* veins indicating sinistral sense of movement. The hammer is ~45 cm long for scale.

The dextral shear zone which strikes between 250° and 270° dominates. Fig. 6a and b shows left-stepping *en echelon* veins indicating dextral shear during their propagation. Individual vein segments show planar geometry, are sub-parallel to each other and generally strike 285°. These veins are crosscut by NW–SE striking veins, see Fig. 4 and Belayneh et al. (2006). Fig. 6c and d shows veins with pinnate geometries. As can be seen from this figure, the through-going shear fracture that links the *en echelon* veins has stepped (staircase) geometry with the longer segments parallel to the tension gashes. Fig. 6e and f shows other left-stepping tension gashes indicating dextral shear with vein geometries ranging between planar and Z-shaped sigmoids. The shear zones have a strike of ~250°. The veins are crosscut by fractures linked to basin inversion and exhumation which began in the Middle Cretaceous. This inversion is the result of the Alpine orogeny caused by the collision between the African and European plates. The resulting regional N–S compression formed the Alpine belt and caused inversion of many of the basins to the northern Europe including the BCB.

The tension gashes shown in Fig. 7 are left-stepping and show straight and pinnate geometries. This shear zone has a strike of 250° and belongs to the same set of shear zones as those shown in Fig. 6. Close inspection of this structure shows that there is a remarkable change in colour of the wall rock along the margin of the shear fracture. The width of this discoloured zone varies between 3 and 5 cm.

The calcite fibres shown in the upper part of Fig. 8a indicate that dextral transtension has occurred along the vein whereas in the lower part an approximately similarly oriented vein contains fibres that indicate an opening mode. The fibres in the upper part of Fig. 8b indicate an opening mode displacement whereas the fibres in the lower part indicate dextral transtension. The continuous dextral transtensional vein shown on the lower left of Fig. 8b grades laterally into left-stepping *en echelon* veins. Both the fibres and the *en echelon* veins indicate a dextral shear component along this zone.

Although, right-stepping arrays of *en echelon* tension gashes showing a sinistral sense of displacement are less commonly developed, they do occur. For example, the oblique fibres in the veins shown in Fig. 9a indicate a sinistral transtension. The vein strikes 295° whereas the fibres are orientated 310°. In Fig. 9b, the fibres in the lower vein also indicate sinistral transtension whereas those in the upper vein, which is sub-parallel to the lower vein, indicate an opening mode failure. The vein in Fig. 9a is part of the complex vein array shown in Fig. 10 and a study of the kinematic indicators (crystal fibres and *en echelon* tension gashes) along this array shows a transition from sinistral transtension to dextral transtension as one moves eastwards, *i.e.* from left to right. Moving eastwards from location A (Fig. 10) the continuous vein containing fibres that indicate sinistral transtension (Fig. 9a) passes laterally into right-stepping, *en echelon* tension gashes (location B, Fig. 10) which are compatible with the sinistral sense of shear indicated by the fibres at location A. Moving further east to location C it is found that the zone-parallel veins are filled with calcite fibres oriented normal to the fracture walls. These indicate opening mode displacement at this location. Continuing eastwards to location D, veins containing calcite fibres indicating dextral transtension are encountered and just to the east at location E they pass laterally into left-stepping, *en echelon* tension gashes which confirm the dextral sense of shear at this position along the zone. There is no consistent crosscutting or abutting relationship of the various structures found along the zone and it is therefore argued that they formed contemporaneously.

On the basis of these observations it is concluded that the stress regime under which basin opening occurred was that of a vertical σ_1, an E–W to WNW–ESE trending *i.e.* basin-parallel, σ_2 and an approximately N–S to NNE–SSW oriented σ_3. This stress field was responsible for the formation of the WNW–ESE trending extensional veins with crystal fibres normal to the fracture walls and is different to the stress regime associated with the formation of the hybrid vein arrays. Here, the orientation of the causative maximum principal compression indicated by the acute bisector of the conjugate hybrid veins (Fig. 5) is parallel to the axis of the basin (E–W to WNW–ESE), σ_2 is vertical and σ_3 ~ NNE–SSW. However, if as is argued by the authors, both sets of veins were associated with basin opening, it is necessary to account for this change in stress field, which involved a switch between σ_1 and σ_2. This proposed change, and the likelihood of it occurring at some stage in the basin opening, are discussed in the following section. Fig. 11 shows the proposed model for the evolution of the Bristol Channel Basin. It can be seen from the figure that the four stages in the evolution of the basin proposed by the previous authors (*e.g.* Peacock and

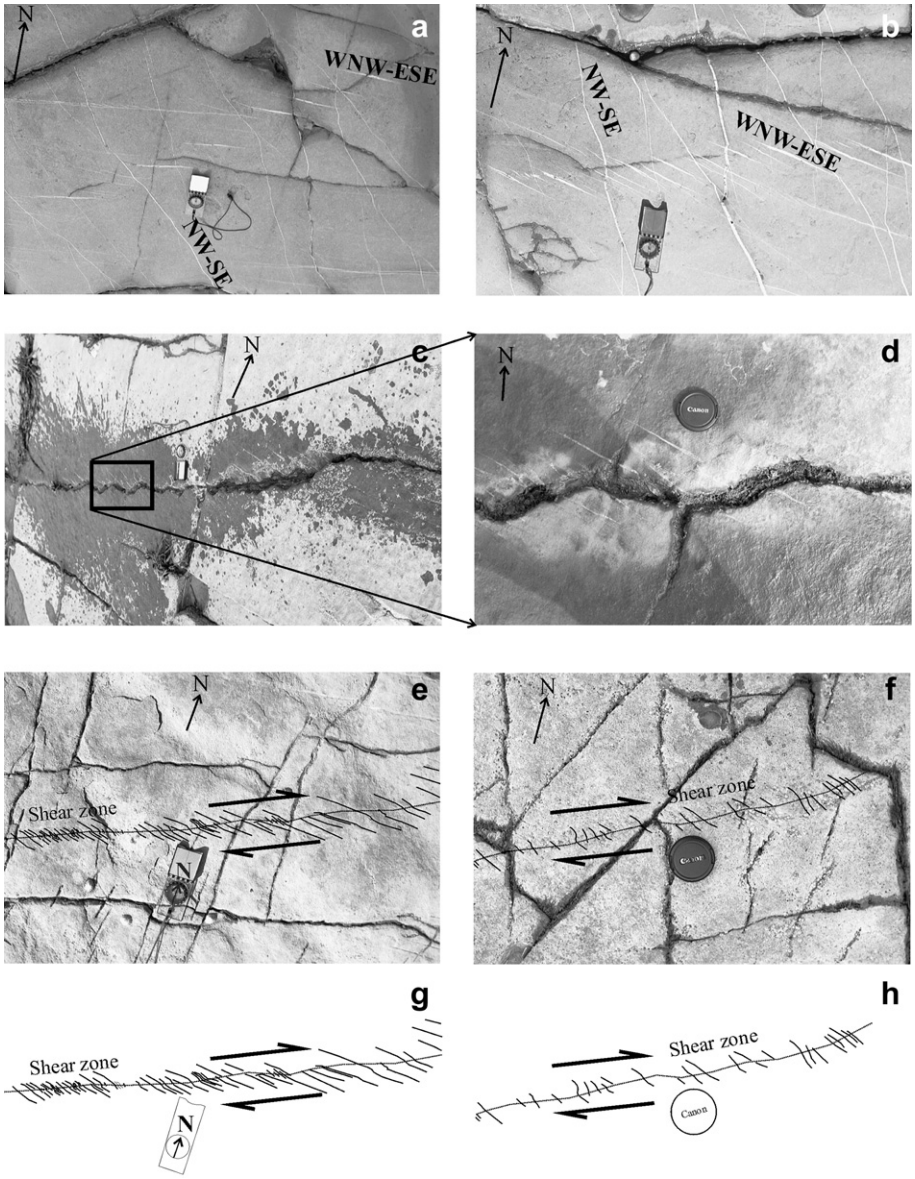

Fig. 6. (a) and (b) Regularly spaced, left-stepping *en echelon* veins and the development of embryonic shear zone, (c) *en echelon* veins showing stepped arrangement that formed as a result of linkage of *en echelon* fractures with the adjacent fracture, (d) enlargement of staircase geometry, (e) and (f) show numerous small-scale left-stepping *en echelon* veins associated with dextral shear zones striking 250°, (g) and (h) are line drawings of (e) and (f), respectively. The compass and camera lens are for scale.

Sanderson, 1999 and Peacock, 2004) can be explained by a single tectonic event involving hybrid failure.

4. Discussions

Two types of fractures are observed in the crust. These are extensional fractures (mode I fractures) termed joints and shear fractures (modes II and III) termed faults. They represent end members of a spectrum of possible brittle failure modes known collectively as hybrid fractures *i.e.* fractures involving components of both extensional and shear failure. The factor that determines whether extensional or shear failure occurs in a rock is the magnitude of the differential stress, *i.e.* the diameter of the Mohr stress circle (see for example Anderson, 1951; Price and Cosgrove, 1990). For extensional failure to occur the differential stress must be less than four times the tensile strength (T) of the rock and for shear failure it should be greater than 4 T (Fig. 1). Fractures that form under the differential stress of ~4 T show characteristics of both extensional and shear displacements. Consequently these fractures are referred to as hybrid fractures or veins (*i.e.* when they are in filled with minerals). The influence of fluid pressure on the evolution of the basin has been discussed by Cosgrove (2001). However, the focus of this paper is that of establishing the magnitude of the differential stress ($\sigma_1 - \sigma_3$) linked to fracturing rather than the absolute fluid pressure linked to fracturing.

Field observations in the study area indicate that wide spread extensional fracturing was associated with the opening of the Bristol Channel Basin. These fractures trend approximately E–W *i.e.* along the axis of the basin. In addition to these extensional fractures, a complex zone of fracturing and veining which runs approximately sub-parallel to the extensional fractures has also been observed (see *e.g.* the discussion related to Figs. 8–10). As noted in the previous section the kinematic indicators associated

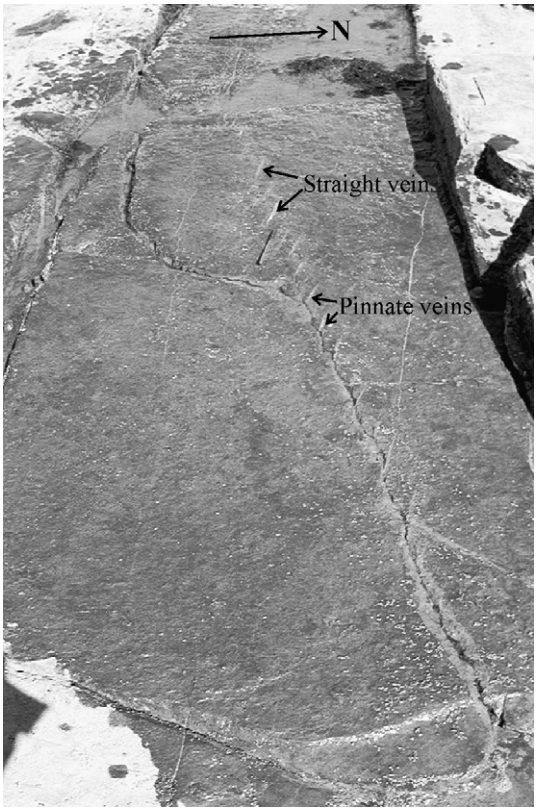

Fig. 7. Left-stepping *en echelon* veins indicating a dextral sense of displacement. Note that there is a remarkable change in colour on both sides of the shear zone. Calcite dissolves from the matrix adjacent to the fracture and precipitates as vein elsewhere.

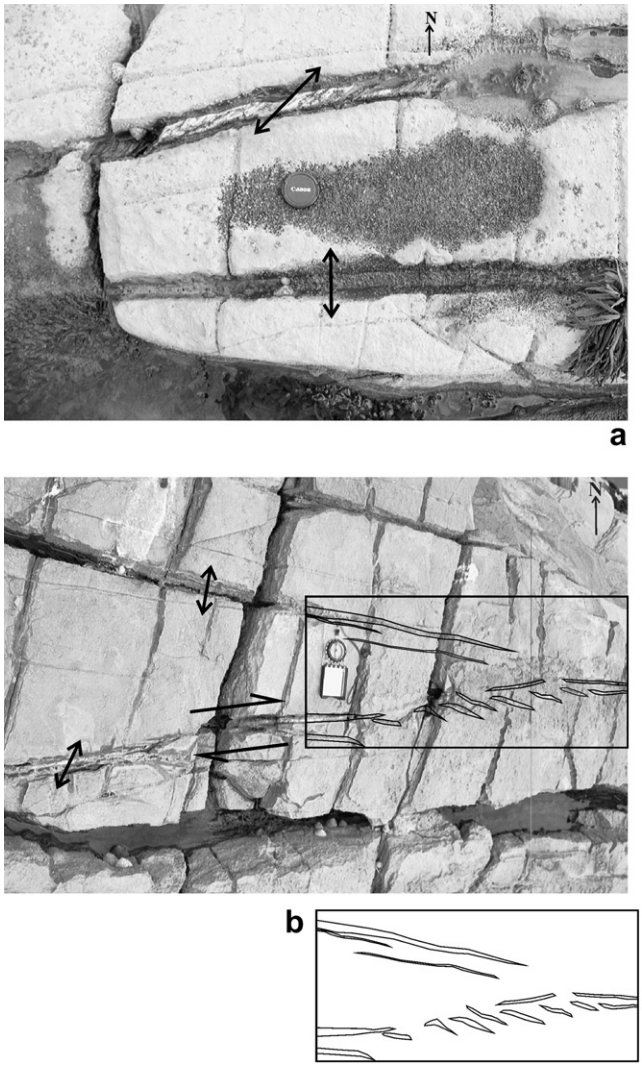

Fig. 8. (a) Plan view of calcite fibres showing a dextral transtension and opening mode displacement in the upper and lower parts of the photograph, respectively. The camera lens is for scale. In (b), the lower right hand side of the photograph, dextral transtension is inferred from calcite fibres and left-stepping *en echelon* tension gashes whereas in the upper part of the photograph, pure opening mode displacements can be deduced. In both photographs the full arrows show the direction of opening and half arrows indicate the sense of displacement of blocks. Highlighted box is shown as line drawing.

with this fracture zone indicate sinistral transtension in one region, pure extension in another and dextral transtension in another. There seems to be no systematic crosscutting relationships between these different kinematic indicators and they therefore appear to have formed synchronously. Previous workers have interpreted these different indicators as indicating a sequence of different deformation events and this has resulted in a complex history of basin opening being proposed (Peacock and Sanderson, 1999; Peacock, 2004). However, as discussed earlier, these apparently contradicting observations which apparently indicate three separate and different episodes of deformations can be unified into a single tectonic event if it is argued that they represent the expression of hybrid failure.

This interpretation has an impact on the stress history of basin opening because it requires that the original stress regime which gave rise to the basin-parallel extension fractures during basin opening (*i.e.* one of a vertical maximum principal stress, WNW–ESE intermediate and NNE–SSW minimum), changed so that the vertical stress becomes the intermediate principal stress and the WNW–ESE stress the maximum. The likelihood of such a stress modification – *i.e.* a switch of σ_1 and σ_2 – will depend on the relative magnitudes of σ_1 and σ_2.

The orientation and magnitudes of the stresses operating during the opening of the BCB have been discussed by previous workers. Peacock and Sanderson (1999) and Peacock (2004) working on the southern margin of the basin inferred a N–S extension for the area between Kilve and Watchet and a more complex history for the Lilstock area (Fig. 3) during basin opening. Nemčok and Gayer (1996) inferred stress states based on data from syn-sedimentary faults for the Upper Triassic and the stress analysis technique of Angelier (1989) for the Early Jurassic. The stress magnitudes inferred for Early Jurassic rifting by Nemčok and Gayer were: $\sigma_1 = 12.98$ MPa, $\sigma_2 = 12.56$ MPa, $\sigma_3 = 8.80$ MPa and it is likely that this small difference between σ_1 and σ_2 continued during basin subsidence. Based on stratigraphic data, Kamerling (1979) derived the subsidence curve for the Bristol Channel Basin and North Somerset area (Fig. 11). This shows that the maximum burial depth occurred during the Lower Cretaceous and was approximately 2.4 km.

As described earlier, although during the initial stages of basin opening, σ_1 was vertical, $\sigma_2 \sim$ E–W and $\sigma_3 \sim$ N–S, in order for the hybrid veins to form it would be necessary for there to be a switch in the orientations of the intermediate and maximum principal stresses. Such a switch is only likely if the difference in the magnitude of the maximum and intermediate principal stresses was small. Fortunately the work of Nemčok and Gayer (1996) confirms that this was the case ($\sigma_1 = 12.98$ MPa, $\sigma_2 = 12.56$ MPa,

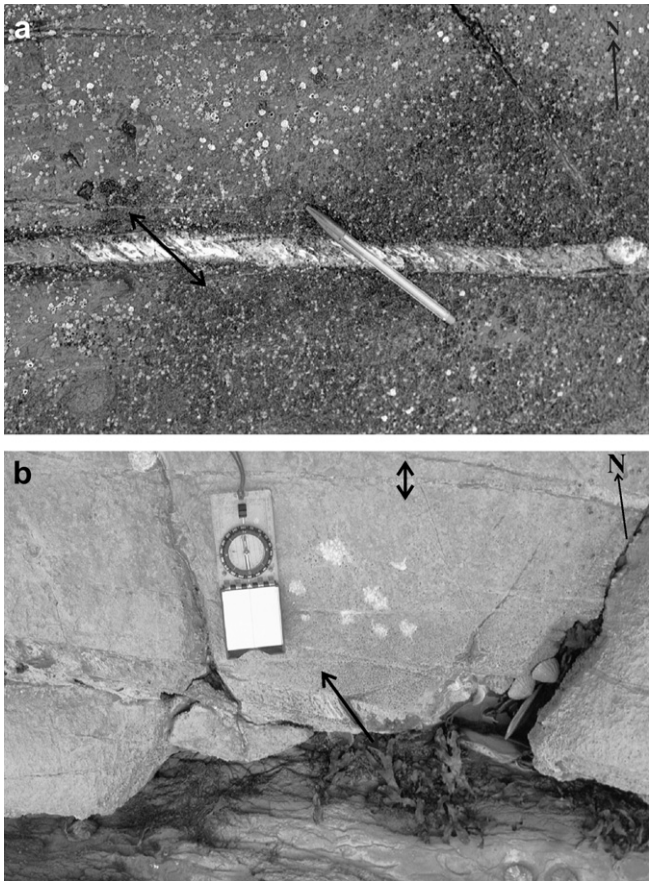

Fig. 9. (a) Calcite fibres are oriented NW–SE showing a sinistral transtensional sense of opening. The pen indicates the direction of displacement. In (b) the fibres in the lower vein indicate sinistral transtension whereas the one in the upper vein indicate pure opening mode.

$\sigma_3 = 8.80$ MPa). It is therefore argued that at some point in the opening of the basin, a switch occurred between σ_1 and σ_2 so that the σ_1 acted along the basin axis (~WNW–ESE) and σ_2 was vertical. It is during this stress regime that the hybrid veins described in this paper are thought to have formed. In the above model we have assumed that basin opening occurred at right angles to the basin bounding faults. However, an alternative model has been proposed to account for compressional structures during basin opening by De Paola et al. (2006). Based on work in the Northumberland Basin, they argue that if the basin opened in transtension, shortening structures could form if the bulk strain undergoes kinematic partitioning (transtensional strain). In this way, these authors were able to simplify a previously proposed more complex deformation history into a single event.

5. Conclusion

The available field data suggest that the Bristol Channel Basin formed as a result of a general N–S directed extension during Permian to Cretaceous times. Early veins (*i.e.* the precursors to the main ~E–W trending basin bounding fault arrays) which, in the study area, formed in Lower Liassic limestones, show dominantly opening mode displacement. However, a complex array of hybrid fractures showing both extensional and shear displacements is found sub-parallel to these extension fractures.

As discussed above, a variety of kinematic indicators occur in association with the hybrid fracture zones, all of which can be explained as the result of a single stress regime. If however, this association is not recognised and the individual indicators interpreted separately, an unnecessarily complex (and incorrect) stress history of basin evolution will result.

As noted earlier, the four stages of basin opening described by Peacock and Sanderson (1999) and Peacock (2004) can be explained by a single event that gave rise to the formation of hybrid veins during basin opening and subsidence.

The proposed model of basin opening requires the stress field associated with the formation of the early formed extensional fractures to change, specifically for there to be a switch of the maximum and intermediate principal stresses, before the formation of the hybrid fractures. Fortunately estimates of the stress magnitudes during basin opening have been made by Nemčok and Gayer who derive values of $\sigma_1 - \sigma_3 \sim 4.2$ MPa, $\sigma_1 - \sigma_2 \sim 0.42$ MPa.

We argue that the close proximity of σ_1 and σ_2 values resulted in a switch between the two at some point in basin opening, and that this, combined with the fact that the differential stress ($\sigma_1 - \sigma_3$) was approximately four times the tensile strength of the rock, resulted in the formation of the ~E–W striking hybrid veins described in this work.

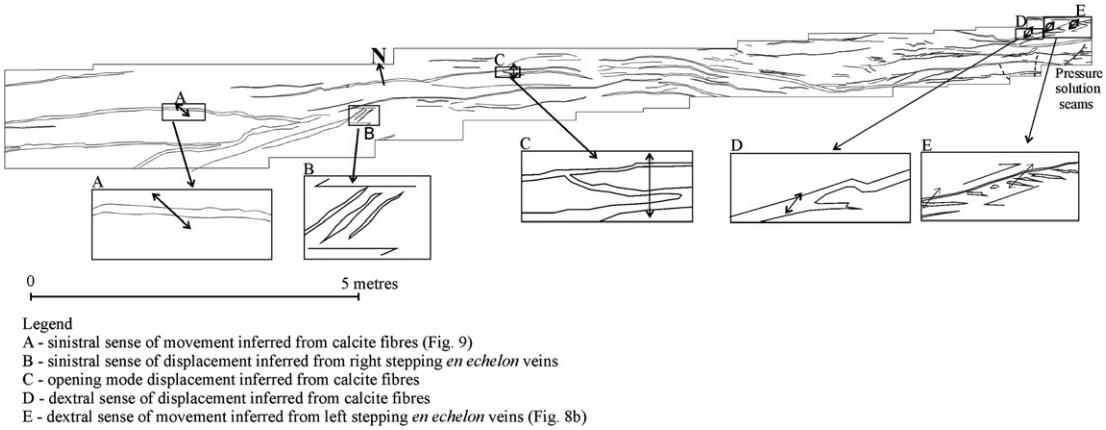

Fig. 10. Line drawing of the veins from a mosaic of photographs showing sinistral transtension (west A) inferred from calcite fibres and right-stepping, locally Z-shaped sigmoidal calcite veins (B). The calcite fibres in veins at C indicates pure opening mode. The calcite fibres in the vein at location D indicate formation under conditions for dextral transtension. The dextral component of shear at this locality is confirmed by the left-stepping *en echelon* veins at E. Full arrows indicate the direction of opening and half arrows the sense of shear.

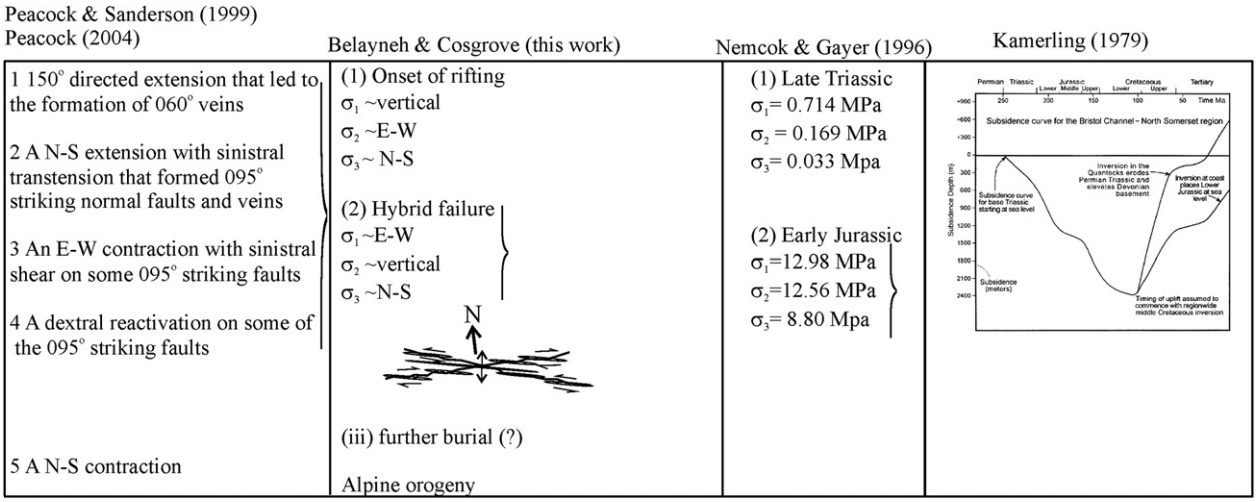

Fig. 11. Proposed models for the evolution of the Bristol Channel Basin.

The identification of hybrid fracture zones sub-parallel to the pure extensional veins which parallel the basin margins, enables a relatively simple model of basin opening to be proposed which it is argued can replace the four stages of basin opening proposed by Peacock and Sanderson (1999) and Peacock (2004).

Acknowledgments

The first author is funded by the Technology Strategy Board (TSB) and industrial sponsors of phase 2 Project under the Industry Training Facilitator (itf): BP, ConocoPhillips, ExxonMobil, Petro-Canada & Total on Improved Simulation of Fractured and Faulted Reservoirs. John Harrison's comments were invaluable in improving the original version of the manuscript. Reviews by Nigel Woodcock and David Peacock significantly improved the manuscript.

References

Al Mahruqi, S.A.S., 2001. Fracture patterns and fracture propagation as a function of lithology. PhD thesis, Imperial College, University of London, 288 pp.
Anderson, E.M., 1951. The Dynamics of Faulting. Oliver & Boyd, Edinburgh.
Angelier, J., 1989. From orientation to magnitudes in palaeostress determinations using fault slip data. Journal of Structural Geology 11, 37–50.
Atkinson, B.K., 1987. Fracture Mechanics of Rock. Academic Press Inc., 527 pp
Bahat, D., 1991. Tectonofractography. Springer, Heidelberg.
Belayneh, M., Cosgrove, J.W., 2004. Fracture pattern variation around a major fold and their implications regarding fracture prediction using limited data: an example from the Bristol Channel Basin. In: Cosgrove, J.W., Engelder, T. (Eds.), The Initiation, Propagation and Arrest of Joints and Other Fractures. Geological Society, London, Special Publication, vol. 231, pp. 89–102.
Belayneh, M., Masihi, M., Matthäi, S.K., King, P.R., 2006. Prediction of vein connectivity using percolation approach: model test with field data. Journal of Geophysics and Engineering 3, 219–229.
Bobich, J.K., 2005. Experimental analysis of the extension to shear fracture transition in Berea Sandstone. Unpublished MSc thesis, Texas A&M University, 52 pp.
Brooks, M., Trayner, P.M., Trimble, T.J., 1988. Mesozoic reactivation of Variscan thrusting in the Bristol Channel area, UK. Journal of the Geological Society 145, 439–444.
Caputo, R., Hancock, P.L., 1999. Crack-jump mechanism and its implications for stress cyclicity during extension fracturing. Journal of Geodynamics 27, 45–60.
Cosgrove, J.W.,1995. The expansion of hydraulic fracturing in rocks and sediments. In: Ameen, M.S. (ed), Fractography: fracture topography as a tool in fracture mechanics and stress analysis. Geological Society, London, Special Publication 92, 187–196.
Cosgrove, J.W., 2001. Hydraulic fracturing during the formation and deformation of a basin: a factor in the dewatering of low-permeability sediments. AAPG Bulletin 85, 737–748.
Dart, C.J., McClay, K., Hollings, P.N., 1995. 3D analysis of inverted of extensional fault systems, southern margin of the Bristol Channel Basin, UK. In: Buchanan, J.G., Buchanan, P.G. (Eds.), Basin Inversion. Geological Society, Special Publication, vol. 88, pp. 393–413.
Davison, I., 1995. Fault slip evolution determined from crack-seal veins in pull-aparts and their implications for general slip models. Journal of Structural Geology 17, 1025–1034.
De Paola, N., Holdsworth, R.E., McCaffrey, K.J.W., Barchi, M.R., 2006. Partitioned transtension: an alternative to basin inversion models. Journal of Structural Geology 28 (2), 333–352.
Durney, D.W., Ramsay, J.G., 1973. Incremental strains measured by syntectonic crystal growth. In: de Jong, K.A., Scholten, R. (Eds.), Gravity Tectonics. Wiley, New York, pp. 67–96.
van Djik, J.P., Bello, M., Toscan, C., Bersani, A., Nardon, S., 2000. Tectonic model and three-dimensional fracture analysis of Monte Alpi, Southern Apennines. Tectonophysics 324, 203–237.
Engelder, T., 1999. Transitional-tensile fracture propagation: a status report. Journal of Structural Geology 21, 1049–1055.
Ferrill, D.A., Wyrick, D., Morris, A.P., Sims, D.W., Franklin, N.M., 2004. Dilational fault slip and pit chain formation on Mars. GSA Today 14 (10). doi:10.1130/1052-5173(2004)014 <4:DFSAPC>2.0.CO:2.
Gillespie, P.A., Howard, C.B., Walsh, J.J., Watterson, J., 1993. Measurement and characterisation of spatial distributions fractures. Tectonophysics 226, 113–141.
Gillespie, P.A., Walsh, J.J., Bonson, C.G., Manzocchi, T., 2001. Scaling relationships of joints and vein arrays from the Burren Co. Clare, Ireland. Journal of Structural Geology 23, 183–201.
Hancock, P.L., 1985. Brittle microtectonics: principles and practice. Journal of Structural Geology 7, 437–457.
Hancock, P.L., 1994. From joints to palaeostress. In: Roure, F. (Ed.), Peri-tethyan Platforms. Technip Editions, Paris, pp. 141–158.
Huang, Q., Angelier, J., 1989. Fracture spacing and its relation to bed thickness. Geological Magazine 126, 355–362.
Hudson, J.A., Priest, S.D., 1979. Discontinuities and rock mass geometry. International Journal of Rock Mechanics, Mining Sciences and Geomechanics Abstract 16, 339–362.
van Hoorn, B., 1987. The South Celtic Sea/Bristol Channel Basin: origin, deformation and inversion history. In: Zeigler, P.A. (Ed.), Compressional Intra Plate deformations in the Alpine Foreland. Tectonophysics, 137, pp. 309–334.
Jolly, R.J.H., Sanderson, D.J., 1995. Variation in the form and distribution of dykes in the Mull swarm. Journal of Structural Geology 17, 1543–1557.
Jolly, R.J.H., Cosgrove, J.W., Dewhurst, D.N., 1998. Thickness and spatial distributions of clastic dykes, northwest Sacramento Valley, California. Journal of Structural Geology 20, 1663–1672.
Kamerling, P., 1979. The geology and hydrocarbon habitat of the Bristol Channel Basin. Journal of Petroleum Geology 2, 75–93.
Marín-Lechado, C., Galindo-Zaldívar, J., Rodríguez-Fernández, L.R., González-Lodeiro, F., 2004. Faulted hybrid joints: an example from the Campo de Dalias (Betic Cordilleras, Spain). Journal of Structural Geology 26, 2025–2037.
Narr, W., Suppe, J., 1991. Joint spacing in sedimentary rocks. Journal of Structural Geology 13, 1037–1048.
Nemčok, M., Gayer, R., 1996. Modelling palaeostress magnitude and age in extensional basins: a case study from the Mesozoic Bristol Channel Basin, UK. Journal of Structural Geology 18, 1301–1314.
Nemčok, M., Gayer, R., Miliorizos, M., 1995. Structural analysis on the inverted Bristol Channel basin: implications for the geometry and timing of fracture porosity. In: Buchanan, J.G., Buchanan, P.G. (Eds.), Basin Inversion. Geological Society, London, Special Publications, vol.88, pp. 355–392.
Nelson, R., 1985. Geologic Analysis of Naturally Fractured Reservoirs. Gulf Publishing Company, Houston, 320 pp.

Nicholson, R., 1991. Vein morphology, host rock deformation and the origin of the fabrics of echelon mineral veins. Journal of Structural Geology 13, 635–641.
Odling, N.E., 1997. Scaling and connectivity of joint systems in sandstones from western Norway. Journal of Structural Geology 19, 1257–1271.
Odling, N.E., Gillespie, P., Bourgine, B., Castaing, C., Chiles, J.-P., Christensen, N.P., Fillion, E., Genter, A., Olsen, C., Thrane, L., Trice, R., Aarseth, E., Walsh, J.J., Watterson, J., 1999. Variations of fracture system geometry and their implications for fluid flow in fractured hydrocarbon reservoirs. Petroleum Geosciences 5, 373–384.
Peacock, D.C.P., 2004. Differences between veins and joints using the example of the Jurassic limestones of Somerset. In: Cosgrove, J.W., Engelder, T. (Eds.), The Initiation, Propagation, and Arrest of Joints and Other Fractures. Geological Society, London, Special Publications, vol. 231, pp. 209–221.
Peacock, D.C.P., Sanderson, D.J., 1999. Deformation history and basin controlling faults in the Mesozoic sedimentary rocks of the Somerset coast. Proceedings of the Geologists Association 110, 41–52.
Pollard, D.D., Aydin, A., 1988. Progress in understanding jointing in the last century. Geological Society of American Bulletin 100, 1181–1204.
Pollard, D.D., Segall, P., 1987. Theoretical displacements and stresses near fractures in rock: with applications to faults joints, veins, dikes, and solution surfaces. In: Aitkenson, B.K. (Ed.), Fracture Mechanics of Rock. Academic Press, pp. 277–349.
Price, N.J., 1966. Fault and Joint Development in Brittle and Semi-brittle Solids. Pergamon Press, Oxford, 170 pp.
Price, N.J., Cosgrove, J.W., 1990. Analysis of Geological Structures. Cambridge University Press, 502 pp.
Priest, S.D., Hudson, J.A., 1976. Discontinuity spacings in rocks. International Journal of Rock Mechanics, Mining Sciences and Geomechanics Abstract 13, 135–148.
Priest, S.D., Hudson, J.A., 1981. Estimation of discontinuity spacing and trace length using scan line surveys. International Journal of Rock Mechanics, Mining Sciences and Geomechanics Abstract 18, 183–197.
van der Pluijm, B.A., Marshak, S., 1997. Earth Structure: an Introduction to Structural Geology and Tectonics. McGraw-Hill, New York.
Ramsay, J.G., 1967. Folding and fracturing in rocks. McGraw-Hill, New York, 568 pp.
Ramsay, J.G., 1980. The crack-seal mechanism of rock deformation. Nature 284, 135–139.
Ramsay, J.G., Huber, M.I., 1987. The Techniques of Modern Structural Geology, Volume 2: Folds and Fractures. Academic Press, London, 576–580 pp.
Ramsay, J.M., Chester, F.M., 2004. Hybrid fracture and the transition from extension fracture to shear fracture. Nature 428, 63–66. doi:10.1038/Nature2333.
Rawnsley, K.D., Peacock, D.C.P., Rives, T., Petit, J.-P., 1998. Joints in the Mesozoic sediments around the Bristol Channel Basin. Journal of Structural Geology 20, 1641–1661.
Rives, T., Razak, M., Petit, J.-P., Rawnsley, K.D., 1992. Joint spacing: analogue and numerical simulations. Journal of Structural Geology 14, 925–937.
Rodriguez, E., 2005. A microstructural study of the extension-to-shear fracture transition in Carrara Marble. Unpublished MSc thesis, Texas A&M University, 62 pp.
Ryan, J.-L., Lonergan, L., Jolly, R.J.H., 2000. Fracture spacing and orientation distributions for two-dimensional data sets. Journal of Geophysical Research 105, 19305–19320.
Sen, Z., Kazi, A., 1984. Discontinuity spacing and RQD estimates from finite length scan lines. International Journal of Rock Mechanics, Mining Sciences and Geomechanics Abstract 21, 203–212.
Sibson, R.H., 1996. Structural permeability of fluid-driven fault-fracture meshes. Journal of Structural Geology 18, 1031–1042.
Sibson, R.H., 1998. Brittle failure mode plots for compressional and extensional regimes. Journal of Structural Geology 20, 655–660.
Sibson, R.H., 2003. Brittle-failure controls on maximum sustainable overpressures in different tectonic regimes. AAPG Bulletin 87, 901–908.
Smith, J.V., 1996. Geometry and kinematics of convergent conjugate vein array systems. Journal of Structural Geology 18, 1291–1300.
Suppe, J., 1985. Principles of Structural Geology. Prentice-Hall, Englewood Cliffs, New Jersey, 537 pp.
Twiss, R.J., Moores, E.M., 1992. Structural Geology. W.H. Freeman & Company, New York, 532 pp.
Urai, J.L., Williams, P.F., van Roermund, H.L.M., 1991. Kinematics of crystal growth in syntectonic fibrous veins. Journal of Structural Geology 13, 823–836.
Vermilye, J.M., Scholz, C.H., 1995. Relation between vein length and aperture. Journal of Structural Geology 17, 423–434.
Wilson, G., 1961. The tectonic significance of small-scale structures and their importance to the geologist in the field. Annales de la Société Géologique de Belgique 84, 424–548.
Woodcock, N.H., Dickson, J.A.D., Tarasewicz, J.P.T., 2007. Transient permeability and reseal hardening in fault zones: evidence from dilation breccia textures. In: Lonergan, L., Jolly, R.J.H., Rawnsley, K., Sanderson, D.J. (Eds.), Fractures Reservoirs. Geological Society, London, Special Publications, vol. 270, pp. 43–53.